13th ewtec 2019
Proceedings of the 13th European Wave and Tidal Energy Conference 1-6 Sept 2019, Naples, Italy

Efficiency of an array of OWC devices equipped with air turbines with pitch control

Dimitrios N. Konispoliatis, Thomas P. Mazarakos, Eirini I. Katsidoniotaki, Antonios K. Vamiadakis, Takvor H. Soukissian, Spyridon A. Mavrakos

***Abstract*—The efficiency of an oscillating water column (OWC) device for offshore wave energy conversion is affected by several parameters related to: a) the climate environmental conditions at the deployment location; b) the hydrodynamic characteristics of the OWC device as they are related to the design of the oscillating chamber; c) the characteristics of the installed air turbine; and d) the device's position in the array relevant to the wave train propagation.**

In practice, the geometry of an OWC is determined for the maximum energy potential sea state. Moreover, the position of the OWC array is fixed at the deployment location, thus the OWC cannot be adapted by itself to maximize the energy absorption at each different sea state. However, the air turbine characteristics in each oscillating chamber can vary rapidly, according to the frequency of the incoming wave, using an air turbine with pitch control.

The examined sea location of the present study is close to Sicily Island at the Mediterranean Sea. The environmental conditions of the examined location are defined by on site wave records. This study presents the methodology for the optimal Wells air turbine design at a given design sea state. Furthermore, passive rotor blade pitch control is investigated for maximizing the performance of the WEC system for several sea states.

***Keywords*—Absorbed Power, Air Turbine, Efficiency, Oscillating Water Column, Pitch Control**

I. Introduction

RENEWABLE Energy Sources (RES) as alternative forms of energy supply are increasingly attracting the global interest since they are inexhaustible, pollution-free reducing the impact on natural environment. Wave energy has one of the highest energy densities among the other RES but the main obstacle in harvesting is the high energy cost. Especially, wave energy potential included in the deep-water waves of the offshore location is much higher than the other forms of wave energy such as shoreline and nearshore wave in addition to the fact that it is easily predictable. However, construction and maintenance of offshore WEC system are expensive and difficult due to the harsh sea conditions. Technological advancements in efficiency of WEC devices play a key role for the development of the offshore wave energy industry. In order to be successful, the Levelized Cost of Energy (LCOE) of wave energy should be competitive among the other technologies thus, research has focused on optimization of the WEC response.

Oscillating Water Column (OWC) technology is one of the first concepts of wave energy conversion. OWCs are mainly located on fixed structures on the shoreline. Applications as a floating device are also possible mainly for offshore locations. A partially submerged structure with an opening in the underwater section is made to trap air above the free air surface. The air inside the internal free

ID No. 1224, Track: Wave device development and testing

This research has been partially financed by the European Union, Horizon 2020, the E.U. Framework Program for Research and Innovation, Research Fund for Coal and Steel, Program: REFOS (709526): Life - Cycle Assessment of a Renewable Energy Multi - Purpose Floating Offshore System.

D.N. Konispoliatis is with the Laboratory for Floating Structures and Mooring Systems, School of Naval Architecture and Marine Engineering, National Technical University of Athens, 9 Heroon Polytechniou Avenue, GR 15773, Greece (e-mail: dkonisp@naval.ntua.gr).

T.P. Mazarakos is with the Laboratory for Floating Structures and Mooring Systems, School of Naval Architecture and Marine Engineering, National Technical University of Athens, 9 Heroon Polytechniou Avenue, GR 15773, Greece (e-mail: tmazarakos@naval.ntua.gr).

E. Katsidoniotaki is with the Laboratory for Hydraulic Turbomachinery, School of Mechanical Engineering, National Technical University of Athens, 9 Heroon Polytechniou Avenue, GR 15773, Greece (e-mail: eirinikatsido@gmail.com) and with the Division of Electricity, Department of Engineering Sciences, Uppsala University, Box 534, 75121, Uppsala, Sweden (e-mail: eirini.katsidoniotaki@angstrom.uu.se).

A. Vamiadakis is with the Laboratory for Floating Structures and Mooring Systems, School of Naval Architecture and Marine Engineering, National Technical University of Athens, 9 Heroon Polytechniou Avenue, GR 15773, Greece (e-mail: vamiadakisantonis@gmail.com).

T.H. Soukissian is with Hellenic Center for Marine Research, 46.7km Athens Sounio Avenue, GR 19013, Greece (e-mail: tsouki@hcmr.gr).

S.A. Mavrakos is with the Laboratory for Floating Structures and Mooring Systems, School of Naval Architecture and Marine Engineering, National Technical University of Athens, 9 Heroon Polytechniou Avenue, GR 15773, Greece (e-mail: mavrakos@naval.ntua.gr) and with the Hellenic Center for Marine Research, 46.7km Athens Sounio Avenue, GR 19013, Greece (e-mail: mavrakos@hcmr.gr).

surface moves according to the oscillatory motion of the water column to drive the Wells turbine placed across. The Wells turbine is an axial-flow air turbine designed to extract energy from ocean waves. The turbine is self-rectifying i.e., produces a unidirectional time-averaged torque from reciprocating flow (see Fig. 1).

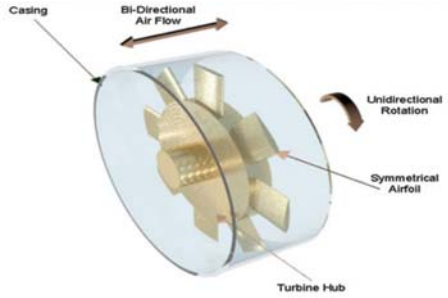

Fig. 1. Schematic configuration of a Wells turbine. Source [1]

The efficiency of an OWC device in an array is affected by several parameters related to: (a) the climate – environmental conditions at the deployment location expressed as significant wave height and peak wave period, for estimation of the resource potential; (b) the hydrodynamic characteristics of the OWC device as they are related to its geometric characteristics (wall thickness, draught, shape of chamber) ([2], [3]); (c) the position of each OWC device regarding to the direction of the wave propagation; (d) the type of the installed air turbine (e.g. Wells-, Savonius-, Dennis- type [4], [5]), the geometry and the pitch angle of the rotor blades [6], [7], developing OWC's efficiency monographs for each air flow rate to the air turbine.

In practice, it is difficult to maximize the efficiency of an OWC array in every wave condition at the deployment site by varying the geometric characteristics of the oscillating chamber or by changing rapidly the position of the OWC device in the array regarding the wave frequency of the incoming wave. However, when the Wells air turbine in the OWC device can change the rotor blade pitch angle, then it is possible control of the pressure difference across the turbine versus flow rate to be achieved. In this way, the energy extracted from the waves can be maximized.

In the present paper the efficiency of an array of floating OWC devices as being described in the REFOS multipurpose floating platform [8] – [9], equipped with air turbines with pitch control is examined. Numerical results of the absorbed power by the REFOS platform are presented for possible deployment site at the Mediterranean Sea based on wave records near Sicily Island.

II. Description of the REFOS Multi – Purpose Power System

The REFOS floating system has been developed for supporting the DTU 10 MW Reference Wind Turbine (WT) [10]. It encompasses an array of three identical OWC devices which can oscillate about their mean equilibrium position moving as a unit in a triangle configuration. Each

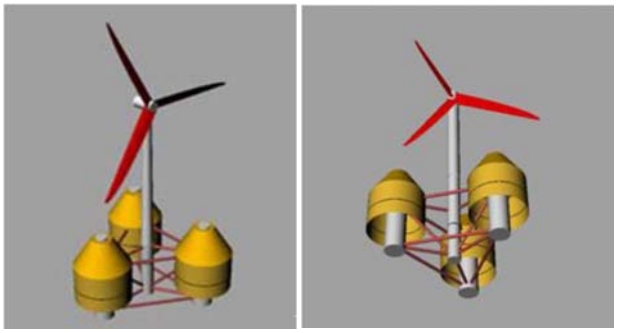

Fig. 2. REFOS Multi-purpose floating structure suitable for offshore wind and wave energy exploitation: above (left side) and below (right side) sea water surface (SWL)

OWC device consists of an exterior partially immersed toroidal oscillating chamber of finite volume supplemented by a concentric interior piston – like truncated cylinder. In the centre of the platform a solid cylindrical body is placed to support the aforementioned WT. The structure which is floating in finite depth waters and it is exposed to the action of regular surface waves, is moored through three tensioned tethers as a TLP platform each one being mounted at the bottom of the concentric interior piston – like truncated cylinder of each OWC device (see Fig. 2). The REFOS structure has been presented thoroughly at [8] – [9] and thus only its basic characteristics of the floater, the moorings and the WT are presented in the below Tables I, II.

TABLE I
REFOS Floating platform and mooring properties

Elevation of main/offset columns above SWL	10.00 m
Spacing between columns	50.00 m
Draught of the structure	20.00 m
Radius of central column, a_c	6.00 m
Radius of inner concentric cylindrical body, a_{in}	7.00 m
Inner radius of the oscillating chamber, a_{ic}	14.0 m
Outer radius of the oscillating chamber, a_{oc}	15.5 m
Oscillating chamber's draught	8.00 m
Diameter of braces	1.60 m
Number of tendons	3
Mooring tendon length	180 m
Mooring tendon diameter	1.22 m
Mooring tendon wall thickness	0.042 m
Pretension per tendon	18838 kN
Line stiffness k_{xx} of each tendon	104 kN/m
Line stiffness k_{zz} of each tendon	173533 kN/m

TABLE II
REFOS 10 MW DTU WT properties

Cut in, Cut out speeds	4 – 25 m/s
Rated wind speed	11.4 m/s
Nominal power	10 MW
Number of blades	3
Rotor diameter	178.3 m
Length of each blade	86.35 m
Total mass of the WT	1200 t

III. CLIMATE CONDITIONS AT THE DEPLOYMENT LOCATION

The selected location for the REFOS platform installation, was considered near Sicily Island (coordinates 37.30° N; 12.69° E) (see Fig. 3) since this area combines high wind and wave potential in 200m water depth. The wave climate at the deployment location can be described through the frequency of occurrence of each pair of spectral peak period T_p and Significant wave height H_s, which is given in Table III. The obtained values refer to the total available sample for the period 1980–2011. In the Table IV, the wind velocity U_w at the examined location is presented regarding the most probable value of the bivariate variable (H_s, T_p). The recording interval at both Tables III and IV is 3 hours [11]. The wave data have been obtained by the ERA-20C data set, published by the European Centre for Medium-Range Weather Forecasts (ECMWF) [12].

Fig. 3. Selected location near Sicily Island, for the REFOS platform installation (Google Earth)

TABLE III
BIVARIATE FREQUENCY TABLE FOR LOCATION 37.30° N; 12.69° E (SOUTH WESTERN PART OF SICILY ISLAND)

Tp (s)	Hs (m)						
	0 – 1	1 – 2	2 – 3	3 – 4	4 – 5	5 – 6	6 – 7
2 – 3	0.014	0.000	0.000	0.000	0.000	0.000	0.000
3 – 4	0.180	0.000	0.000	0.000	0.000	0.000	0.000
4 – 5	**0.240**	0.022	0.000	0.000	0.000	0.000	0.000
5 – 6	0.150	0.076	0.001	0.000	0.000	0.000	0.000
6 – 7	0.084	0.082	0.016	0.000	0.000	0.000	0.000
7 – 8	0.017	0.037	0.026	0.003	0.000	0.000	0.000
8 – 9	0.006	0.012	0.012	0.007	0.001	0.000	0.000
9 – 10	0.001	0.002	0.003	0.004	0.002	0.000	0.000
10 – 11	0.000	0.000	0.000	0.000	0.001	0.000	0.000
11 – 12	0.000	0.000	0.000	0.000	0.000	0.000	0.000

The cell (H_s, T_p) with the highest frequency of occurrence is shown in boldface digits.

TABLE IV
MOST PROBABLE VALUES OF (H_s, T_p) AND SUBSAMPLES' SIZE FOR VARIOUS BINS OF U_w

U_w (m/s)	2-4	4-6	6-8	8-10	10-12	12-14	14-16	16-18	18-20
H_s (m)	0.335	0.756	0.865	1.335	1.982	2.830	3.824	4.897	6.186
T_p (s)	2.821	3.610	4.542	5.404	6.596	6.396	8.556	8.848	10.28
Subs size	30024	22419	17505	11100	6040	2479	806	184	27

IV. COUPLED HYDRO – AERO –ELASTIC ANALYSIS

Details of the hydrodynamic analysis within the context of potential theory formulation for an array of OWC devices that are floating either independently or as a unit can be found in [13] and [14]. For completeness, below a short introduction to the theory behind the hydro – aero dynamic problem is presented.

The group of 4 bodies (3 OWC devices and 1 vertical cylindrical body supporting the WT) is excited by a plane periodic wave of amplitude $H/2$, frequency ω and wave number k propagating in water of finite water depth d. It is also assumed small amplitude, inviscid, incompressible and irrotational fluid flow, so that linear potential theory can be employed. A global Cartesian co-ordinate system O-XYZ with origin on the sea bed and its vertical axis OZ directed positive upwards is used. Moreover, three local cylindrical co-ordinate systems (r_q, θ_q, z_q), q = 1, 2, 3 are defined with origins on the sea bottom and their vertical axes pointing upwards.

The velocity potential around the q = 1, 2, 3, 4 device/ body (three OWCs at the vertices of the triangular floater and the vertical central cylindrical body that supports the WT), can be decomposed as in [13]:

$$\Phi^q(r,\theta,z;t) = \mathrm{Re}[\varphi^q(r,\theta,z)\cdot \mathrm{e}^{-\mathrm{i}\omega t}] =$$
$$= \mathrm{Re}\left[\left[\varphi_0^q + \varphi_7^q + \sum_{p=1}^{4}\sum_{j=1}^{6} \dot{x}_{j0}^{p}\,\varphi_j^{qp} + \sum_{p=1}^{3} p_{in0}^{p}\,\varphi_p^{qp}\right]\cdot e^{-i\omega t}\right] \quad (1)$$

Here, φ_0^q is the velocity potential of the undisturbed incident harmonic wave, φ_7^q is the scattered potential around the q device, when it is considered fixed in waves with the duct open to the atmosphere, φ_j^{qp} is the motion – dependent radiation potential around the body q resulting from the forced oscillation of the p body in j direction with unit velocity amplitude, $\dot{x}_{j0}^{p}$, (j = 1, 2,…,6), and air chambers of both p and q devices being considered open to the atmosphere. The subscript j stands for surge (j = 1), sway (j = 2), heave (j = 3), roll (j = 4), pitch (j = 5) and yaw (j = 6) modes of motions, respectively. Moreover, φ_p^{qp} is the pressure – dependent radiation potential around the q body when it is considered open to the atmosphere (i.e. atmospheric air pressure inside its chamber) due to unit time harmonic oscillating pressure head, p_{in0}^{p}, in the chamber of the p device when devices q and p are considered fixed in otherwise calm water.

The potentials φ_j^q (j= 0, 7; q = 1, 2, 3, 4), φ_j^{qp} (j= 1, …, 6; q, p = 1, 2, 3, 4) and φ_p^{qp} (q = 1, 2, 3, 4; p = 1, 2, 3) are solutions of Laplace's equation in the entire fluid domain and satisfy the following boundary conditions:

$$\omega^2 \varphi_j^q - g \frac{\partial \varphi_j^q}{\partial z} = 0 \quad (2)$$

for $r_{1,2,3} \geq a_{oc}$ and $a_{in} \leq r_{1,2,3} \leq a_{ic};\ r_4 \geq a_c; j = 0, 7$

$$\omega^2 \varphi_j^{qp} - g \frac{\partial \varphi_j^{qp}}{\partial z} = 0 \quad (3)$$

for $r_{1,2,3} \geq a_{oc}$ and $a_{in} \leq r_{1,2,3} \leq a_{ic};\ r_4 \geq a_c; j = 1,2,..,6$

$$\omega^2 \varphi_P^{qp} - g \frac{\partial \varphi_P^{qp}}{\partial z} = \begin{Bmatrix} 0 & \text{for } r_{1,2,3} \geq a_{oc} \\ -\delta_{q,p} \dfrac{i\omega}{\rho} & \text{for } a_{in} \leq r_{1,2,3} \leq a_{ic} \end{Bmatrix} \quad (4)$$

at the outer and inner free sea surface z=d of each body and the zero normal velocity on the sea bed (z=0). Furthermore, the potentials have to fulfil kinematic conditions on the mean body's wetted surface, and also a radiation condition must be imposed ensuing that propagating disturbances must be outgoing. Finally, the velocity potentials and their derivatives must be continuous at the vertical boundaries of neighbouring fluid regions [13].

Following the method of separation of variables for the differential Laplace equation, appropriate expressions for the velocity potentials in each fluid domain can be derived. These expressions satisfy the corresponding conditions at the horizontal boundaries of each fluid region and the radiation condition at infinity in the outer fluid domain. Moreover, the velocity potentials have been constructed in such a way that their homogeneous parts can be reduced to simple Fourier series representations at the vertical boundaries of the various fluid regions. Applying the kinematic conditions at the device's vertical walls and the requirement for continuity of the potential and its radial derivative at the vertical boundaries of neighbouring fluid domains the system of equations for the unknown Fourier coefficients is obtained. Methods for the solution of the diffraction and the motion–, pressure– radiation problems have been extensively reported in previous works ([13], [14]) and, so, they are no further elaborated here.

Having determined the partial velocity potentials in each fluid region, the hydrodynamic forces on the hull of the REFOS floater (exciting forces, hydrodynamic added mass and damping coefficients, pressure hydrodynamic forces) can be calculated. The gravitational, inertial and aerodynamic loads that the WT contributes on the floater dynamics are defined in the simplest possible way, with respect to gravitational and inertial loading, the wind turbine is modeled as a collection of concentrated masses, namely the masses of the blades, the nacelle, the hub and the tower. Applying the Lagrange equations, the dynamic equations of the WT can be reduced to the 6 degrees of rigid body motions of the floating supporting structure, in the following linearized form [9], [15], [16]:

$$\sum_{j=1}^{6} \left[-\omega^2 \left(M_{i,j}^{WT} + \frac{i}{\omega} B_{i,j}^{WT} \right) + C_{i,j}^{WT} \right] \cdot q = Q \quad (5)$$

Here q denote the vector of the 6 floater motions. The RHS contains gravity, buoyancy as well as the aerodynamic part that corresponds to the reference state, while the mass matrix $M_{i,j}^{WT}$ includes the WT inertia (including the gyroscopic effects due to the rotation), the damping matrix $B_{i,j}^{WT}$ includes the WT damping due to rotation and aerodynamics and finally the stiffness matrix $C_{i,j}^{WT}$ includes the contribution from both aerodynamics and gravity.

The investigation of the dynamic equilibrium of the forces acting on the floating structure leads to the following well–know system of differential equations of motions, describing the couple hydro–aero–elastic problem of the investigated floating supporting structure in the frequency domain [15], [16]:

$$\sum_{j=1}^{6} \left[-\omega^2 \left(M_{i,j} + M_{i,j}^{WT} + A_{i,j} + \frac{i}{\omega} B_{i,j} + \frac{i}{\omega} B_{i,j}^{WT} \right) + C_{i,j} + \right.$$
$$\left. + C_{i,j}^{WT} \right] \cdot X_{j0} = F_i \,, i = 1,2, \ldots, 6 \quad (6)$$

The superscript *WT* corresponds to physical quantities associated to the wind turbine. Moreover, $M_{i,j}$ and $C_{i,j}$ are elements of the mass and stiffness matrix of the floating structure, $A_{i,j}$, $B_{i,j}$, represent its 6 by 6 added mass and damping matrices, respectively, F_i is the six by one vector that contains the hydrodynamic exciting forces on the floating supporting structure and the forces due to air pressure inside the oscillating chamber, and X_{j0}, is the motion displacement of the entire system at the j–th direction with respect to the global co-ordinate system G.

V. Design of the Air Turbine

A. Wells air turbine characteristics

A Wells air turbine is assumed to be placed in each device's duct between the chamber and the outer atmosphere. Assuming isentropy so that variations of air density and pressure are proportional to each other with $c_{air}^2 = \frac{dp_{in0}^i}{d\rho_{air}}$, c_{air} being the sound velocity in air and p_{in0}^i the inner air pressure distribution inside the chamber of each OWC i =1, 2, 3, each air turbine can be represented by a pneumatic complex admittance Λ [17]:

$$\Lambda^i = \frac{q^i}{p_{in0}^i} = \left[\frac{KD}{\rho_{air} N} + (-i\omega) \frac{V_0}{c_{air}^2 \rho_{air}} \right] \quad (7)$$

Here, q^i is the air volume flow through the air turbine of the i = 1, 2, 3 device, whereas N is the rotational speed of turbine blades, D the outer diameter of turbine rotor, ρ_{air} the static air density and V_0 the device's air chamber volume. The empirical coefficient K depends on the design, the setup and the number of turbines. The real part of Λ is related to the pressure drop through the turbine,

whereas the imaginary part of Λ represents the effect of air compressibility inside the OWCs chamber.

The mean absorbed power by each OWC device i = 1, 2, 3 of the REFOS platform can be written as [18]:

$$P^i = \frac{1}{2} Re\left[\Lambda \cdot (p_{in0}^i)^2\right] \quad (8)$$

Following [19] remarks, when the Wells pneumatic admittance Λ of an OWC restrained in the wave impact and in isolation condition, equals to an optimum coefficient Λ_{opt}, the absorbed power by the OWC device reaches its maximum value. In Fig. 4 this optimum coefficient Λ_{opt} of a restrained in the waves, single OWC device, same as the OWCs at the REFOS platform, is depicted against the wave frequency, whereas in Fig. 5 the total absorbed power by the three OWC devices of the REFOS platform, as derived by Eq. 8, is presented for the above Λ_{opt} coefficient.

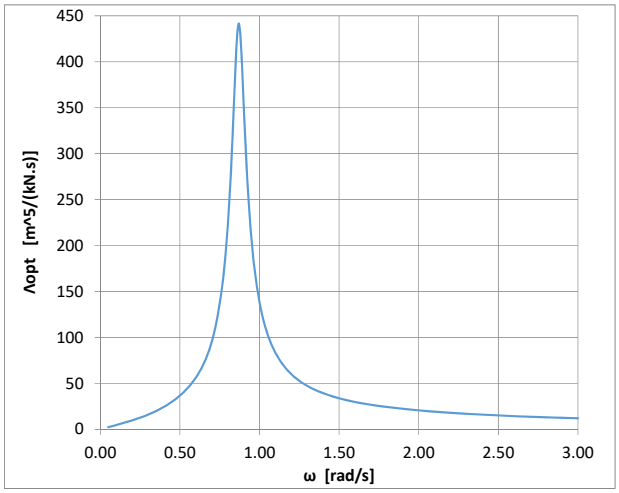

Fig. 4. Wells pneumatic admittance Λ_{opt} versus wave frequency ω

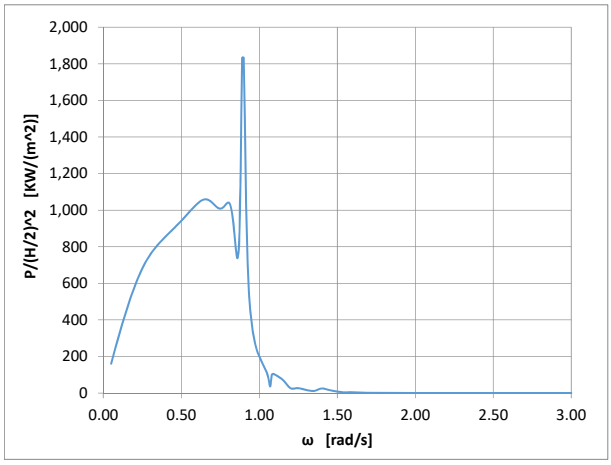

Fig. 5. Total absorbed power by the three OWC devices versus wave frequency ω

It can be obtained from Fig. 4, that since the Λ_{opt} coefficient is a function of the wave frequency, in order to absorb maximum power by the OWC devices of the REFOS platform, the Wells turbine pneumatic admittance of each OWC device, Λ^q, should be equal to the Λ_{opt} value, meaning that each Wells turbine should vary its characteristics (see Eq. 7) for every wave frequency. However, due to construction limitations on the design of the Wells turbine (i.e. diameter of the rotor, rotation speed etc.) regarding the incoming wave characteristics, a Wells turbine (without pitch control) was selected initially to operate at its optimum Λ_{opt} value in a single wave frequency where the absorbed power by the OWC is maximum.

Following Table III, which depicts the frequency of occurrence of each cell at the deployment location, Table V of the total absorbed power from the REFOS platform can be derived as a function of each cell (H_s, T_p) for Λ_{opt} turbine coefficient.

TABLE V
TOTAL ABSORBED POWER (KW) BY THE REFOS PLATFORM FOR EACH WAVE CONDITION

Tp (s)	*Hs* (m)						
	0.5	1.5	2.5	3.5	4.5	5.5	6.5
2.5	0.00	0.00	0.00	0.00	0.00	0.00	0.00
3.5	0.03	0.27	0.75	1.47	2.43	3.63	5.07
4.5	1.45	13.05	36.25	71.05	117.45	175.45	245.05
5.5	4.84	43.53	120.90	236.97	391.73	585.18	817.31
6.5	18.57	167.15	464.31	910.04	1504.3	2247.2	3138.7
7.5	56.03	504.24	1400.6	2745.3	4538.1	6779.2	9468.5
8.5	63.20	568.80	1580	3096.8	5119.2	7647.2	10680
9.5	66.38	597.43	1659.5	3252.6	5376.8	8032.1	11218
10.5	64.76	582.83	1618.9	3173.2	5245.4	7835.8	10944
11.5	61.88	556.91	1546.9	3032	5012.2	7487.3	10457

Multiplying the frequency of each cell (H_s, T_p) (i.e. Table III) by total absorbed power by the REFOS platform in each cell (H_s, T_p) (see Table V), the total absorbed power percentage in each wave condition is depicted in Table VI.

TABLE VI
TOTAL ABSORBED POWER PERCENTAGE BY THE REFOS PLATFORM FOR EACH WAVE CONDITION

Tp (s)	*Hs* (m)						
	0.5	1.5	2.5	3.5	4.5	5.5	6.5
2.5	0.00	0.00	0.00	0.00	0.00	0.00	0.00
3.5	0.01	0.00	0.00	0.00	0.00	0.00	0.00
4.5	0.35	0.28	0.00	0.00	0.00	0.00	0.00
5.5	0.73	3.31	0.08	0.00	0.00	0.00	0.00
6.5	1.56	13.66	7.59	0.00	0.00	0.00	0.00
7.5	0.97	18.72	**36.94**	7.03	0.10	0.00	0.00
8.5	0.35	6.99	19.06	22.39	3.22	0.08	0.00
9.5	0.07	1.08	4.20	11.92	12.94	1.42	0.00
10.5	0.00	0.15	0.57	1.23	3.01	2.94	0.97
11.5	0.00	0.00	0.00	0.07	0.00	0.25	0.35

The cell (H_s, T_p) with the largest value is shown in boldface digits

It can be shown in Table III that the cell (H_s, T_p) with the highest frequency of occurrence is (0-1m; 4-5s). However, from Table VI, it can be seen that the cell with the largest total absorbed power percentage is the (2.5m; 7.5s) (i.e. cell with boldface digits). Therefore, in order the OWCs to maximize their efficiency, the installed Wells air turbine should be designed for the above wave conditions (i.e. (2.5m; 7.5s). Thus, from Figure 4 the Λ^q coefficient equals to 343.848 m^5/(kN.s), meaning that from the analysis in Section IV (see also Eq. 7), $q^i = 512\, m^3/s$ and $p_{in0}^i =$

$1.490kPa$, for i=1,2,3, referred at the water – air interface inside each OWC.

B. Design of the air turbine

The Wells air turbine converts the pneumatic energy in the OWC chamber to mechanical energy. For improving the efficiency performance of the OWC wave energy device, it is essential that the turbine is matched with the OWC hydrodynamic characteristics as far as the pressure drop and air volume flow is concerned (see Eq. 7).

The analysis of the turbine's performance is based on the Radial equilibrium approach and Actuator Disc Theory [20, 21] with two dimensioning cascade data based on small – scale experiments and numerical predictions. In applying both methods to the Wells turbine, the flow is divided into angular rings and each ring is treated as a two dimensional cascade with a 90° stagger. Next, by implementing Bernoulli's principle on the aforementioned values of (q^i, p^i_{in0}) for the i = 1,2,3 device (see Eq. 7), the corresponding values of design conditions $(q^i_2, p^i_{in0_2})$ are calculated at the inlet of the turbine (at the top of the OWC). In the present contribution it is assumed that the same Wells air turbine is placed in the three OWCs of the REFOS platform, regardless their position to the wave impact. The design methodology presented here is an iterative procedure [21]. The output of each iteration is compared with the design requirements of the Wells turbine (air flow rate, pressure drop across the turbine). The interactive procedure is performed at all the stages in the design methodology until predictions from the analysis compares well with the design requirements within certain acceptable limits (see Fig 6). An algorithm has been developed in the MATLAB® environment following the 6 steps of the methodology described below:

Step 1: Initially, the value of outer rotor diameter (D_{tip}) and Hub to Tip ratio (h) parameter (see Fig. 7) are assumed in order to estimate the absolute air velocity V_2 and the pressure p_{in0_2}, i.e.:

$$V_2 = \frac{q_2}{\frac{\pi D^2_{tip}}{4}(1-h^2)} \tag{9}$$

The pressure at the turbine's inlet (on the top of OWC) is computed by Bernoulli's equation:

$$p_{in0} + \rho_{air} g H_1 + \frac{1}{2}\rho_{air} V_1^2 = p_{in0_2} + \rho_{air} g H_2 + \frac{1}{2}\rho_{air} V_2^2 \tag{10}$$

Here H_1 is the height of the OWC bottom opening to water free surface, H_2 is the height of the OWC opening on the top to water free surface, V_1 the air velocity at the water surface, and V_2 the air velocity at the OWC opening on the top.

Step 2: The relation between the air flow ratio φ and incident angle of air α on the blade is defined as:

$$\alpha = tan^{-1}\varphi \tag{11}$$

It is worth noticing here, that the air flow ratio φ is a measure of air flow incidence to the blades of the turbine.

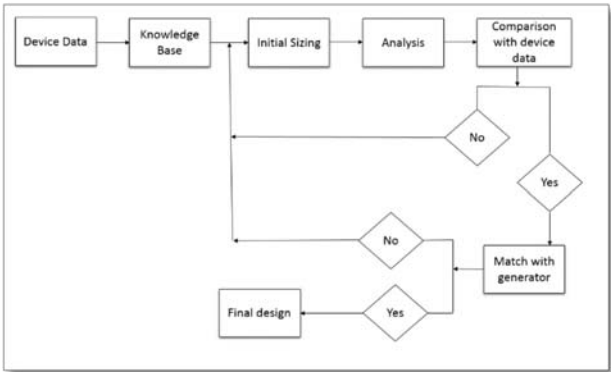

Fig. 6. Block diagram of the design methodology

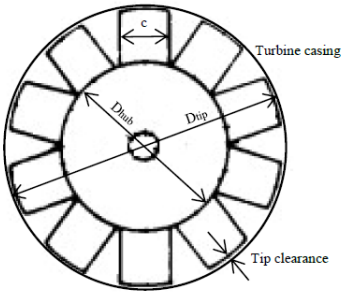

Fig. 7. Design of a Wells turbine blade

For a given rotor speed, the flow ratio φ is proportional to the air flow rate. The flow ratio for the design point of a Wells turbine has to be within a range from 0.13 to 0.20 corresponding in an air flow incidence from 7.4° to 11.3°. At this step we select a value of air flow ratio within this range.

Step 3: Now the circumferential velocity at the tip of the blade, U_t, is calculated along with the Mach number, which should be less than the critical value (Ma_{cr} < 0.5) [20, 21].

$$\varphi = \frac{V_2}{U_t} \rightarrow U_t = \frac{V_2}{\varphi} = \Omega \cdot \frac{D_{tip}}{2} \tag{12}$$

$$\left[Ma = \frac{U_t}{a}\right] \leq Ma_{cr} \tag{13}$$

Here Ω is the turbine rotational speed [rad/s].

Step 4: The Reynolds number, which in real practice installations is recommended to be greater than 10^6, is defined as:

$$Re = \frac{U_t \cdot c}{\nu} \tag{14}$$

Where ν is the kinematic viscosity of air ($1.51 \cdot 10^{-5}$ m²/s) and c is the blade cord (see Fig. 7).

At this step, the designer sets the restrain of Reynolds accepted range.

Step 5: The value of Solidity (σ) is assumed taking into account that it is recommended a value less than 0.5 for monoplane Wells turbine. Then, the Eq. (15) gives the number of turbine's blades:

$$\sigma = \frac{N \cdot c}{\pi \cdot \frac{D_{tip}}{2}} \tag{15}$$

Where N are the number of blades, c the blade cord and D_{tip} the outer rotor diameter (see Fig. 7).
Usually a Wells turbine consists of 4 to 8 blades [20, 21], therefore if the value of N is not a realistic number, then the Reynolds number or/ and solidity value have to be re-assigned.

Step 6: The pressure drop across the rotor is estimated by [20, 21]:

$$P_{2p} = \frac{N \cdot c \cdot \rho \cdot w^2}{4 \cdot \pi \cdot D_{tip}/2} \left[\frac{C_D}{sina} + C_T cota) \right] \quad (16)$$

Here w the relative air velocity, a angle of air incidence at the turbine inlet, C_D, C_T drag and torque coefficient depending on the airfoil profile.

The Wells turbine with geometrical characteristics as defined above is acceptable when the results from Eqs. (10) and (16) have converged, otherwise, the designer changes the values of outer rotor diameter, Hub to Tip ratio, solidity, Reynolds number. The iterative procedure is continued until the convergence is achieved.

In the REFOS case, at the installation location the design requirements as far as the airflow rate and the pressure head are: $q^i = 512\ m^3/s$ and $p_{in0}^i = 1.490 kPa$. Therefore, it is proposed two Wells turbines placed in parallel on the top of the housing to be installed in each OWC. The characteristics of the selected Wells turbine (without pitch control) are presented in Table VII.

TABLE VII
WELLS TURBINE CHARACTERISTICS IN PARALLEL INSTALLATION FOR THE REFOS PLATFORM

Parameters	Symbol	Design
Outer Rotor Diameter (m)	D_{tip}	5.10
Hub to Height Ratio	h	0.50
Reynolds Number	Re	$7 \cdot 10^6$
Critical Mach number	Ma_{cr}	0.50
Solidity	σ	0.29
Chord at blade tip (m)	c	1.16
Number of blades	N	4

In Figs. 8 and 9 the static pressure, the mechanical power output and the efficiency are presented versus the air flow rate. It can be seen from Figs 8 and 9 that in the pre-stall region (approximately airflow rate $330\ m^3/s$) there is a linear slope between pressure drop across the blade and airflow rate. The reason for this behavior is that at higher values of air flow rate, the boundary layer on the airfoil blades tends to and subsequently does fully separate, increasing the drag and reducing the lift. According to Computational Fluid Dynamic (CFD) analysis (ANSYS® Fluent software), the Wells turbine has 180 kW mechanical power output and the efficiency is nearly 60%, whereas the airflow operating range is up to 330 m³/s. After this value of air flow rate the incipient of stall occurs and the torque and efficiency of turbine drop significantly.

C. *Air turbine with variable pitch*

In the above subsections A and B the optimum Wells air turbine characteristics in the OWC devices of the REFOS platform have been determined in order to maximize the

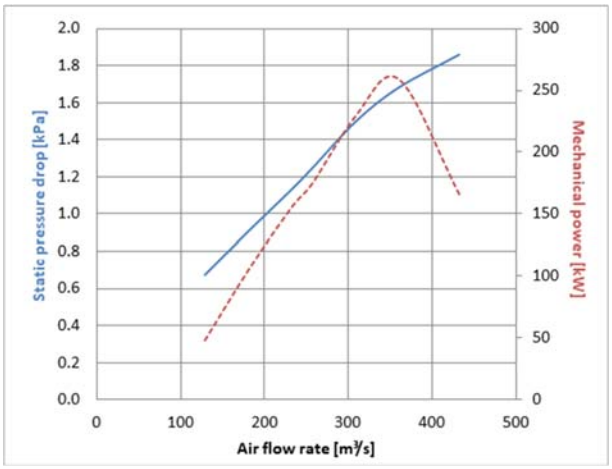

Fig. 8. Static pressure and mechanical power for airflow rates

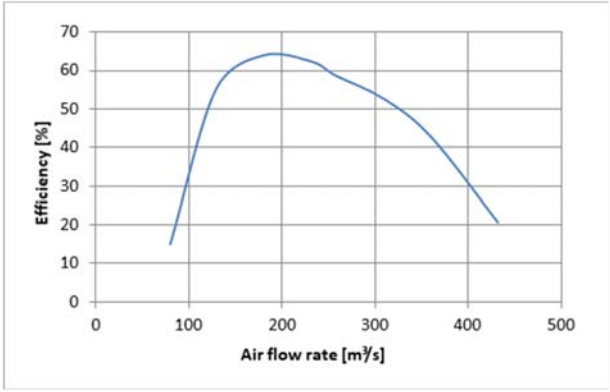

Fig. 9. Efficiency for airflow rates

absorbed wave power at a specific wave peak period Tp = 7.5 s (or ω= 0.83 rad/s) (see discussion on Table VI). In the sequel, the aforementioned Wells air turbine has been replaced by an air turbine with same characteristics but with rotor blades which can be set at varying angle during turbine's operation, aiming at maximizing the amount of energy extracted from the waves in wider range of wave frequencies. That is to say that, variable pitch control is a method of tuning for maximum absorption of the pneumatic energy captured by OWC. Moreover, under irregular wave conditions, Wells turbine can avoid the incipient of stall on the rotor blades via pitching control.

In fact, there is a strong relation between the angle of incidence of air to the rotor blade and the turbine's efficiency. Thus, changing the blade pitch, the angle of air incidence can be adjusted in order to set the turbine operate in the high-performance region. Moreover, the occurrence of stall, which drops the efficiency instantaneously, is avoided. For small angles (and small flow coefficients), the blade lift force component in the direction of blade motion is of the order of the drag force and the efficiency is poor or even negative, on the other hand, aerodynamic stalling is the limiting factor for increasing flow coefficient and is responsible for the drop in efficiency [22].

In Fig. 10 the steady state pressure versus the air flow numerical results, of a modified Wells turbine for various

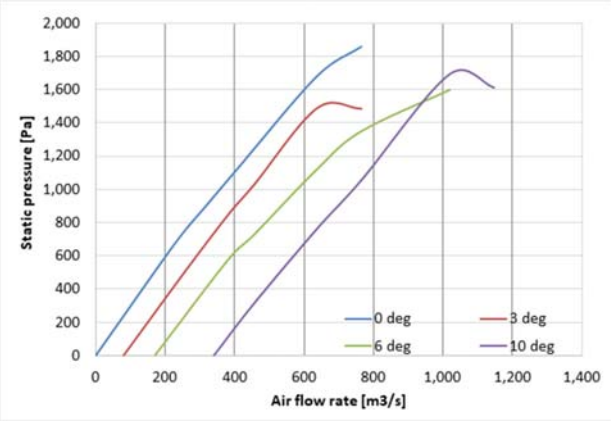

Fig. 10. Static pressure for various pitch angles

pitch angles as have been investigated by numerical simulation via CFD analysis, are presented. Increasing the pitch angle pushes the curve to the right delaying stall to higher flow rates. In addition, the rate $\frac{q}{p_{ino}} = \Lambda$ (see Eq. 7) increases, with the increase of the pitch angle. It is evident from Fig. 10 that for pitch angles 3, 6 and 10 degrees the Λ coefficient equals approx. to 428; 566; 834, respectively whereas for zero angle equals to 343.848 $m^5/(kN.s)$ (see also subsection B), meaning that when the pitch angle is increasing the inner air pressure is decreasing.

Nevertheless, comparing the obtained Λ values for each pitch angle (see Fig. 10), with the values of Λ_{opt}, see Fig. 4, it is observed that the latter reaches values up to 450 $m^5/(kN.s)$. Therefore, only the 3 degrees angle case (i.e. 428 $m^5/(kN.s)$ leads to an increase of the OWC efficiency comparing to the Wells air turbine without pitch variation, see subsection B. On the other hand, the 6 and 10 degrees pitch angles cases will not increase the OWC efficiency comparing to its corresponding counterpart for air turbine without variable pitch, since the Λ_{opt} coefficient (see Fig. 4) doesn't reach 566; 834 $m^5/(kN.s)$ values, at any wave frequency.

VI. Absorbed Power

In order to assess the absorbed wave power by the REFOS multipurpose floating structure, for the four aforementioned air turbine parameters (i.e. 0, 3, 6, 10 pitch angle degrees) in the Mediterranean Sea (see Section III), the Jonswap spectrum provided by [23] is applied at the Eq. (8).

TABLE VIII
ABSORBED WAVE POWER FROM THE REFOS PLATFORM FOR AIR TURBINE WITH BLADE ANGLES 0, 3, 6, 10 DEGREES

H_s (m)	0.335	0.756	0.865	1.335	1.982	2.830	3.824	4.897	6.186
T_p (s)	2.821	3.610	4.542	5.404	6.596	6.396	8.556	8.848	10.28
P_0 (MWh)	0.000	0.000	0.003	0.061	0.561	1.028	3.232	5.367	6.945
P_3 (MWh)	0.000	0.000	0.003	0.058	0.535	0.978	2.949	4.816	6.096
P_6 (MWh)	0.000	0.000	0.002	0.052	0.488	0.889	2.562	4.107	5.089
P_{10} (MWh)	0.000	0.000	0.002	0.043	0.407	0.739	2.027	3.182	3.863

Here the subscript i of the absorbed power P_i denotes the blade angle, i.e. 0, 3, 6, 10.

In the Table VIII, the absorbed wave power from the OWC devices, is presented against the most probable values of (H_s, T_p) at the deployment location (see Table IV). Here, the Wells air turbine is assumed without pitch control, at a fixed blade angle of 0, 3, 6, 10 degrees. It is evident that the REFOS system absorbs more wave power for the case of 0 degrees pitch blade angle compared to its corresponding counterpart for the remaining pitch blade angles.

In the sequel, the absorbed wave power by the REFOS platform in the deployment location is presented using the aforementioned air turbine with pitch control. The air turbine can vary its characteristics (i.e. the Λ coefficient value) by varying its blade angle (i.e. 0, 3, 6, 10 degrees) depending on the wave frequency of the incoming wave, in order the Λ coefficient value to be as close as possible to the Λ_{opt} which maximizes the system's efficiency.

In Fig. 11 the total absorbed wave power from the OWC devices per year when using air turbines with pitch control is presented against the corresponding absorbed power by the REFOS system utilizing air turbines without pitch control at zero degrees blade angle. A small increase of the absorbed wave power when using a Wells with pitch control can be established. However, the amount of the increase is low since as aforementioned only the 3 degrees blade angle have a positive effect on the REFOS efficiency.

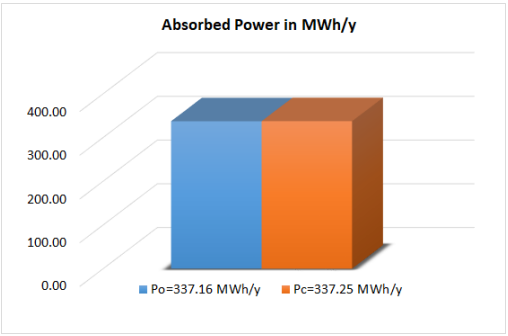

Fig. 11. Absorbed power per year, P_i, from the REFOS platform. Here P_o is the absorbed power without pitch control (i.e. zero degrees blade angle) and P_c is the absorbed power with pitch control (i.e. the blade angle varies from 0 to 10 degrees)

VII. Conclusion

In the present paper the design of a Wells air turbine for an array of OWC devices as being described in the REFOS multipurpose floating structure is presented. Initially, the air turbine is assumed without pitch control, and its characteristics are optimized to maximize the absorbed power by the devices at a specific wave frequency of the incoming wave. This frequency is selected in such a way that the absorbed wave power by the REFOS platform will be maximized at a specific wave frequency at the deployment location in the Mediterranean Sea

In the sequel, the aforementioned air turbine is examined to operate with pitch control depending on the wave frequency of the incoming wave. The purpose is the

characteristics of the air turbine in each wave condition to be as close as possible to their optimum value counterpart which maximizes the system's efficiency.

It has been presented that the pitch control mechanism of an air turbine increases the efficiency of the OWC. However, the benefits of the pitch control were not utilized to all the blade angles (i.e. 3, 6, 10 degrees), but only for a blade angle up to 3 degrees. This is because the initial design of the air turbine in the OWC chambers concerned a Wells turbine without pitch control, with Λ characteristic value that maximizes the absorbed wave power by the REFOS system, Λ being equal to the Λ_{opt} value. This value, though, was tending to the global maximum value of the Λ_{opt} for all wave frequencies in the wave spectrum. As a result, when the blade angle rises above the 3 degrees, the air pressure inside the chambers decreases, therefore the air turbine characteristic Λ value ended to be well above its optimum counterpart.

REFERENCES

[1] A.S., Shehata, et al. "Wells turbine for wave energy conversion: a review," *International Journal of Energy Research* 41.1: pp. 6-38, 2017.

[2] YMC, Delaure, A., Lewis. "3D hydrodynamic modelling of fixed oscillating water column wave power plant by a boundary element methods," *Ocean Engineering* 30; pp. 309–330, 2003.

[3] J.W., Weber, G.P., Thomas. "An investigation into the importance of the air chamber design of an oscillating water column wave energy device," in the *11th International Offshore and Polar Engineering Conference, Stavanger, Norway*; 2001, vol. 1, pp. 581-588.

[4] D.G., Dorrell, W., Fillet. "Investigation of a small scale segmented oscillating water column utilizing a Savonius rotor Turbine," in the *International Conference on Energy and Environment*, Malaysia; 2006, pp. 23–32.

[5] Mohammed Faizal, M.R., Ahmed, Y.H. Lee. "On utilizing the orbital motion in water waves to drive a Savonius rotor," *Renewable Energy*; Vol. 35, pp. 164–169, 2010.

[6] A.F.O., Falcao, P.A.P., Justino. "OWC wave energy devices with air flow control," *Ocean Engineering* 26; pp.1275–1295, 1999.

[7] C., Josset, A.H., Clement. "A time-domain numerical simulator for oscillating water column wave power plants," *Renewable Energy* 32; pp. 1379–1402, 2007.

[8] D.N., Konispoliatis, T.P., Mazarakos, T.H., Soukissian, S.A., Mavrakos, "REFOS: A multi - purpose floating platform suitable for wind and wave energy exploitation**",** *in the 11th International Conference on Deregulated Electricity Market Issues in South Eastern Europe* (DEMSEE 2018), Nicosia**,** Cyprus.

[9] T., Mazarakos, D., Konispoliatis, D., Manolas, S., Voutsinas, S., Mavrakos. "Modelling of an offshore multi-purpose floating structure supporting a wind turbine including second-order wave loads," *in the 11th EWTEC 2015*, Nantes, France.

[10] C., Bak, F., Zahle, R., Bitsche, T., Kim, A., Yde, L.C., Henriksen, A., Natarajan, M.H., Hansen. "Description of the DTU 10 MW Reference Wind Turbine; DTU", in the *Wind Energy Report*-I-0092, 2013.

[11] REFOS: Life-Cycle Assessment of a Renewable Energy Multi-Purpose Floating Offshore System, 42 months program (1/7/2016 – 31/12/2019), Funding EU, Research Fund for Coal and Steel, Grant Agreement No 709256. – REFOS - RFSR – 2015.

[12] ERA-20C Project (ECMWF Atmospheric Reanalysis of the 20th Century). Research Data Archive at the National Center for Atmospheric Research, Computational and Information Systems Laboratory. http://dx.doi.org/10.5065/D6VQ30QG

[13] D.N., Konispoliatis, S.A., Mavrakos, "Hydrodynamic analysis of an array of interacting free–floating oscillating water column devices," *Ocean Engineering*, vol. 111, pp.179–197, 2016.

[14] D.N., Konispoliatis, T.P., Mazarakos, S.A., Mavrakos, "Hydrodynamic an analysis of three-unit arrays of floating annular oscillating-water-column wave energy converters", *Applied Ocean Research*; vol. 61, pp. 42–64, 2016.

[15] T.P., Mazarakos, S.A., Mavrakos, D.N., Konispoliatis, S., Voutsinas, D., Manolas, "Frequency domain analysis for a coupled hydro- aero- elastic behavior of a moored multi-purpose floating structure", in *the COCONET Workshop for Offshore Wind Farms in the Mediterranean and Black Seas,* Hellenic Center of Marine Research, Anavyssos, Greece, 2014.

[16] T.P., Mazarakos, D.N., Konispoliatis, D., Manolas, S.G., Voutsinas, S.A., Mavrakos, "Coupled hydro – aero – elastic analysis of a multi – purpose floating structure for offshore wind and wave energy sources exploitation," in the *12th International Conference on Stability of Ships and Ocean Vehicles* (12th STAB), 2015. Glasgow, Scotland, UK.

[17] H., Martins–rivas, C.C., Mei, "Wave power extraction from an oscillating water column along a straight coast", *Ocean Engineering*; 36, pp. 426–433, 2009.

[18] J., Falnes, P., McIver, "Surface wave interactions with systems of oscillating bodies and pressure distributions", Applied Ocean Research; **7**. pp. 225–234, 1985.

[19] D.V., Evans, R., Porter, "Efficient calculation of hydrodynamic properties of O.W.C type devices", *OMAE* – Volume I – Part B, 1996; pp. 123–132.

[20] L.M.C., Gato, A.F.O., Falcao, **"**On the theory of the Wells turbine," *Trans. ASME,* 1984.

[21] S., Raghunathan, "A methodology for Wells turbine design for wave energy conversion." Proceedings of the Institution of Mechanical Engineers, Part A: Journal of Power and Energy: pp 221-232, 1995.

[22] L.M.C., Gato, L. R. C. Eça, A.F.O., Falcao, "Performance of the Wells turbine with variable pitch rotor blades," *Journal of Energy Resources Technology*: pp. 141-146, 1991.

[23] DNV, 2007, Environmental Conditions and Environmental Loads, Recommended Practice DNV-RP-C205.